American Mineralogist, Volume 76, pages 743–755, 1991

Local equilibrium in metasomatic processes revisited: Diffusion-controlled growth of chert nodule reaction rims in dolomite

RAYMOND JOESTEN
Department of Geology and Geophysics, 345 Mansfield Road, The University of Connecticut, Storrs, Connecticut 06269-2045, U.S.A.

ABSTRACT

Zoning in reaction rims of talc-calcite (TC-CC) and tremolite-calcite (TR-CC) between quartz (Q) and dolomite (DO) is modeled using a system of constrained mass balance equations that describe local buffer equilibria among mineral phases and diffusing components at layer contacts. Chemical potential gradients that drive diffusion of CaO, MgO, and SiO_2 across monomineralic and two-phase layers are established by invariant and univariant buffer equilibria at layer contacts. The structures Q|TC|TC + CC|DO and Q|TR|TR + CC|DO are stable for ratios of Onsager diffusion coefficients in the range $10^{-6} \leq L_{MgOMgO}/L_{SiO_2SiO_2} \leq 10^4$ and $10^{-3} \leq L_{CaOCaO}/L_{SiO_2SiO_2} \leq 10$. Growth of the structure Q|TC|TC + CC|DO involves counterdiffusion of MgO and SiO_2, whereas growth of Q|TR|TR + CC|DO involves diffusion of CaO across the TR layer in addition to diffusion of MgO and SiO_2. The structures Q|TC + CC|DO and Q|TR + CC|DO, analogous to natural examples, appear to be stabilized at $10^{-6} \geq L_{MgOMgO}/L_{SiO_2SiO_2}$ where SiO_2 is the only diffusing component. The structure Q|TC|CC|DO is stable for $L_{MgOMgO}/L_{SiO_2SiO_2} \geq 10^4$ and involves diffusion of MgO. Q|TR|CC|DO appears to be stable over the same range of L-ratio as Q|TR|TR + CC|DO. The latter is probably the stable structure because it possesses the smaller value of the dissipation function for a given set of L-ratios. It is shown that determination of the number of perfectly mobile components for a layer cannot be used to predict the number of diffusing components.

LOCAL EQUILIBRIUM IN METASOMATIC PROCESSES REVISITED

Thompson's paper, "Local Equilibrium in Metasomatic Processes" (1959), provided the foundation upon which essentially all modern work on mass transport in metamorphic rocks is built. Even though a great deal of controversy and misunderstanding followed his discussion of the definition of components and their use in the application of the phase rule to open systems (Weill and Fyfe, 1964, 1967; Korzhinskii, 1966, 1967; Thompson, 1970; Rumble, 1982), his discussion of the role of local equilibrium in the development of zoning in mineral assemblages in binary systems by metasomatic reaction has withstood the test of time. In that discussion, he stressed that (1) reaction between incompatible assemblages and consequent diffusion-controlled growth of intervening product assemblages produces a series of sharply bounded mineral-assemblage layers, each in local equilibrium with its neighbors, and that (2) metasomatic processes produce high-variance assemblages consisting of a small number of phases. Because his arguments were based on consideration of phase equilibria alone, and did not consider the kinetic effects of unequal component mobilities, he did not fully explore the factors that determine the sequence of mineral-assemblage layers that develop in ternary systems and in those of higher order. Thus, he did not recognize the existence of conditions under which multiphase layers are stable in the steady state. The chert-dolomite examples presented here illustrate the role of the relative magnitudes of the fluxes of the diffusing components in determining the sequence and identity of mineral-assemblage layers in structures produced by metasomatic reaction. This work is firmly rooted in Thompson's ideas on local equilibrium and the buffering of chemical potentials by layer-contact mineral assemblages (Thompson, 1959, 1970) and is offered as an expression of thanks to him for the challenge and inspiration he has provided throughout my career.

LOCAL EQUILIBRIUM IN CONCENTRICALLY ZONED NODULES OF CALC-SILICATE

Metamorphism of chert nodules in limestone or dolomite produces structures consisting of concentric shells of calc-silicate minerals around a quartz core. They are natural analogues of the model systems used by Thompson (1959) to illustrate the role of local equilibrium in the buffering of chemical potentials at the contacts of mineral-assemblage layers, which establish the gradients that drive element exchange and the diffusion-controlled growth of layered structures.

0003–004X/91/0506–0743$02.00

Diffusion zoning in a binary system

Reaction rims on chert nodules in limestone form a series of monomineralic layers from quartz core to calcite-rim (Tilley and Alderman, 1934; Tilley, 1942; Reverdatto, 1970; Joesten, 1974; Joesten and Fisher, 1988) that represent the sequence of phases encountered along the join CaO-SiO_2 (projected from CO_2) at the P-T-X_{CO_2} of metamorphism.

For example, calc-silicate nodules from the inner part of the Christmas Mountains contact aureole have the layer sequence quartz|wollastonite|tilleyite|calcite, representing the sequence of phases encountered along the CaO-SiO_2-(CO_2) join in the mineral facies stable in the range 940–1000 °C at 325 bars and $X_{CO_2} \geq 0.35 \pm 15$ (Joesten, 1974, 1983).

Zoned calc-silicate nodules in limestone are the direct natural counterparts of the layered structure quartz|enstatite|forsterite|periclase used by Thompson (1959) to illustrate local equilibrium in a binary system, and his model has proved successful in explaining their growth (Joesten, 1974). Note, however, that several generalizations that follow from the analysis of binary systems do not hold for ternary systems and those of higher order:

1. The identity and sequence of mineral-assemblage layers produced by reaction and local equilibrium in a multicomponent system cannot be predicted from the phase diagram alone, because their bulk compositions need not lie along a compositional join (Thompson, 1959).

2. Mineral-assemblage layers developed along gradients in chemical potential in a multicomponent system need not be monomineralic (Frantz and Mao, 1975, 1979; Joesten, 1977). The only constraint imposed by local equilibrium at layer contacts is that each growing mineral-assemblage layer must be at least univariant at fixed P-T-X_{CO_2}. That is, the gradient of at least one of the chemical potentials of the components comprising the phases of the layer must be independently variable. A growing layer in a system described by N components may thus contain no more than $N - 1$ phases.

3. The buffering of chemical potentials by $N - 1$ or fewer phases in local equilibrium at a layer contact will not be invariant at fixed P-T-X_{CO_2}, so that thermochemical calculation of differences in chemical potential across the adjoining layers can be accomplished only in special cases.

Analysis of the mineral assemblage zoning developed around chert nodules in dolomite serves to illustrate these points and provides a useful tutorial on the methods available for the analysis of diffusion-controlled growth of layered structures.

Diffusion zoning in a ternary system

Reaction rims on chert nodules in dolomite produced by progressive contact metamorphism, ranging in grade from the talc zone to the forsterite zone, have been described by Tilley (1948, 1951) and by Hoersch (1981) from the contact aureole of the Beinn an Dubhaich granite on the Isle of Skye, Scotland and by Moore and Kerrick (1976) from the aureole of the Alta granodiorite stock, Utah. Chert nodules with a quartz or diopside core and rhythmically banded rims of calcite-forsterite in brucite or periclase marble have been described from Beinn an Dubhaich (Tilley, 1951), from the aureole of the Kaizukui-yama granite, Japan (Suzuki, 1977), and from an inclusion in the Santa Olalla tonolite, Spain (Puga and Fontboté, 1980). The interpretation of the evolution of mineral assemblage zoning in these natural examples is complicated (1) by overprinting of mineral assemblages, which is caused by reaction between phases within a growing layer and within the impure chert core with rising temperature, and (2) by the effects of the buffering of fluid composition to different values at nodule cores and rims (Hoersch, 1981). It is assumed in all calculations presented below that (1) reactant dolostone and chert are composed of pure dolomite and quartz, respectively, (2) an intergranular H_2O-CO_2 fluid phase is present, and (3) rapid diffusion of H_2O and CO_2 in the fluid phase maintains a constant value of X_{CO_2} throughout the model structure. The simple models for nodules in the talc zone and tremolite zone developed here do not address the compositional complexities in natural examples. They do provide, however, the basis for the understanding of the mechanism of nodule growth by focusing on those features that are the result of component redistribution driven by diffusion down gradients in chemical potential imposed by metamorphic reaction and consequent local equilibrium at nodule core, rim, and interior mineral-assemblage layer contacts.

Initiation of Growth of Reaction Rims on Chert Nodules in Dolomite

The heating of nodular chert in dolostone to temperatures of 300 to 390 °C at 500 bars in the presence of an H_2O-rich fluid ($X_{CO_2} < 0.7$), as in the contact aureole of the Beinn an Dubhaich granite, or to 350–420 °C at 1 kbar and $X_{CO_2} < 0.7$ as in the Alta aureole, produces reaction rims bearing calcite and talc that separate quartz and dolomite by the reaction

$$\underset{\text{dolomite}}{3CaMg(CO_3)_2} + \underset{\text{quartz}}{4SiO_2} + H_2O = \underset{\text{talc}}{Mg_3Si_4O_{10}(OH)_2} + \underset{\text{calcite}}{3CaCO_3} + 3CO_2. \quad (1)$$

Similarly, the heating of nodular chert in dolostone to temperatures of 390 to 425 °C at 500 bars or to 420–460 °C at 1 kbar in the presence of a CO_2-rich fluid ($X_{CO_2} > 0.7$) produces reaction rims containing calcite and tremolite that separate quartz and dolomite by the reaction

$$\underset{\text{dolomite}}{5CaMg(CO_3)_2} + \underset{\text{quartz}}{8SiO_2} + H_2O = \underset{\text{tremolite}}{Ca_2Mg_5Si_8O_{22}(OH)_2} + \underset{\text{calcite}}{3CaCO_3} + 7CO_2. \quad (2)$$

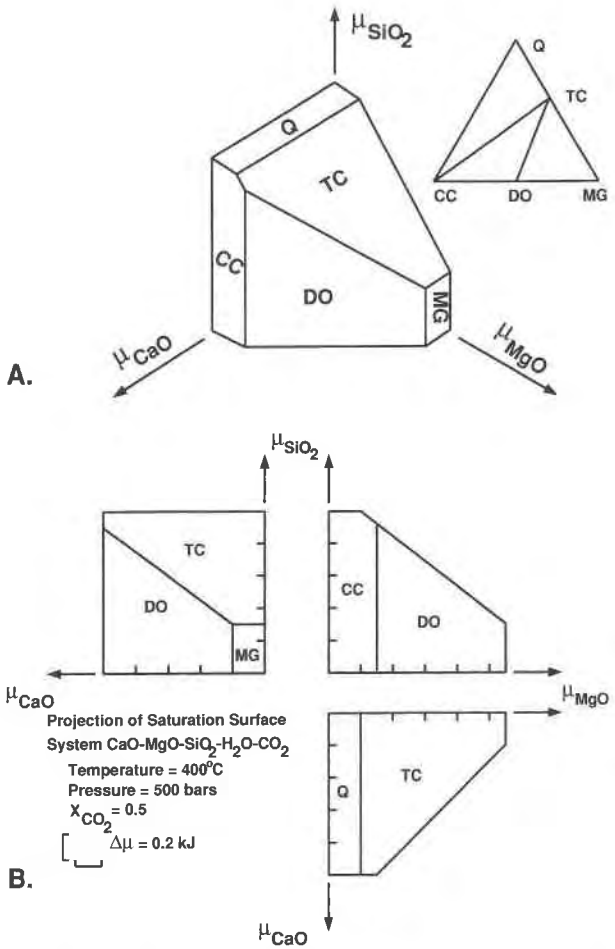

Fig. 1. Saturation surface in μ_{CaO}-μ_{MgO}-μ_{SiO_2} space for the mineral facies produced by breaking the dolomite-quartz tie line by Reaction 1 in the system CaO-MgO-SiO_2-H_2O-CO_2. Chemical potentials computed with thermochemical data of Helgeson et al. (1978) and the MRK model of Holloway (1977) and Flowers (1979) at 400 °C, 500 bars, and X_{CO_2} = 0.5 and normalized to μ_{CaO} = 1.0 for calcite saturation, μ_{MgO} = 1.0 for magnesite saturation, and μ_{SiO_2} = 1.0 for quartz saturation. (**A**) The μ_{CaO}-μ_{MgO}-μ_{SiO_2} surface for the mineral facies shown in the inset. (**B**) Projections of the saturation surface of **A** along axes of μ_{Mgo}, μ_{CaO}, and μ_{SiO_2}.

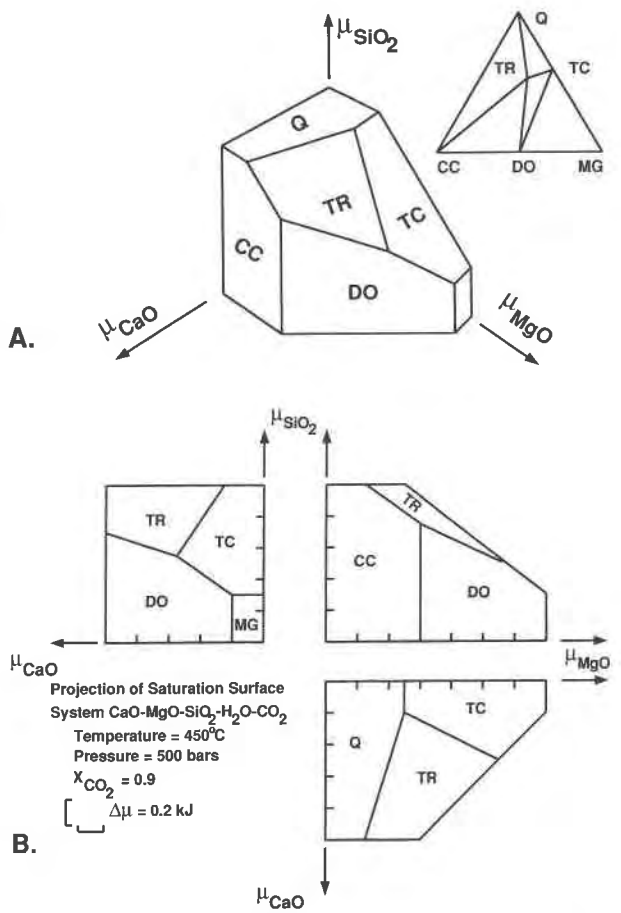

Fig. 2. Saturation surface in μ_{CaO}-μ_{MgO}-μ_{SiO_2} space for the mineral facies produced by breaking the dolomite-quartz tie line by Reaction 2 in the system CaO-MgO-SiO_2-H_2O-CO_2. Chemical potentials computed at 450 °C, 500 bars, and X_{CO_2} = 0.9, as in Figure 1. (**A**) The μ_{CaO}-μ_{MgO}-μ_{SiO_2} surface for the mineral facies shown in the inset. (**B**) Projections of the saturation surface of **A** along μ_{MgO}, μ_{CaO}, and μ_{SiO_2} axes.

Reaction at the contact of a chert nodule enveloped by dolomite initially produces a layer of talc + calcite (TC + CC) by Reaction 1 or of tremolite + calcite (TR + CC) by Reaction 2, separating incompatible quartz (Q) and dolomite (DO). Local equilibrium across the layer contacts, Q|TC + CC and TC + CC|DO or Q|TR + CC and TR + CC|DO, buffers the chemical potentials of CaO, MgO, and SiO_2 (μ_{MgO}, μ_{CaO}, and μ_{SiO_2}) at values that are invariant at a given P-T-X_{CO_2}. Local equilibrium therefore establishes the chemical-potential gradients that drive the exchange of CaO, MgO, and SiO_2 between quartz and dolomite to supply the layer-contact reactions that govern growth of the product layer.

Isothermal-isobaric saturation surface for CaO-MgO-SiO_2-H_2O-CO_2

Phase equilibria, illustrated on the mineral facies diagrams, that result from breaking of the quartz-dolomite tie line by Reactions 1 or 2 are mapped from composition space (inset, Figs. 1A and 2A) onto the saturation surface in chemical potential space, its reciprocal counterpart (Figs. 1A and 2A), using the Gibbs-Duhem equation for each of the phases (Grant, 1977). Three-phase triangles are mapped as invariant points at fixed P-X-T_{CO_2}, whereas two-phase assemblages are univariant lines, and a single phase is represented as a divariant surface within which the values of two of the three chemical potentials are independently variable.

Each μ_i-μ_j diagram in Figures 1B and 2B is the projection of the saturation surface along the third μ axis. Variance on the binary projections is the same as in μ_{CaO}-μ_{MgO}-μ_{SiO_2} space. The bounding edges of the μ_{CaO}-μ_{SiO_2} diagram

are the traces of the saturation surfaces for calcite and quartz, whereas the μ_{Mgo}-μ_{SiO_2} diagram is bounded by the quartz, talc, and magnesite saturation surfaces and the μ_{CaO}-μ_{MgO} diagram is bounded by the calcite, dolomite, and magnesite surfaces. The projected μ_i-μ_j diagrams are topologically identical to $\log_{10}a_i - \log_{10}a_j$ diagrams on which buffered solubility data are portrayed (compare Fig. 2B with Figs. 6J and 9 in Walther and Helgeson, 1980 or Fig. 10 in Walther, 1983, which show the same mineral facies).

Local equilibrium, chemical potential buffering, and diffusion paths

Initial reaction at the boundary of a chert nodule in dolomite may be envisioned to produce a layer of talc + calcite (Reaction 1) or tremolite + calcite (Reaction 2) separating quartz and dolomite. Local equilibrium across the layer contacts, Q|TC + CC and TC + CC|DO, buffers μ_{MgO}, μ_{CaO}, and μ_{SiO_2} at the invariant points on the saturation surface Q + TC + CC and TC + CC + DO, thus establishing the chemical-potential gradients across the TC + CC layer that drive the exchange of MgO and SiO_2 between quartz and dolomite and supply the layer-contact reactions governing growth of the product layer. Note that μ_{CaO} is fixed across the structure by the presence of calcite, and it is assumed that P, T, and X_{CO_2} are constant throughout the structure. Similarly, local equilibrium at the Q|TR + CC and TR + CC|DO layer contacts buffers μ_{MgO}, μ_{CaO}, and μ_{SiO_2} at the Q + TR + CC and TR + CC + DO invariant points (Fig. 2a).

For the system CaO-MgO-SiO_2-H_2O-CO_2 at constant P-T-X_{CO_2}, the three-phase assemblages at layer contacts, Q|TC + CC and TC + CC|DO or, at higher temperature, Q|TR + CC and TR + CC|DO, are invariant buffers of the values of μ_{CaO}, μ_{MgO}, and μ_{SiO_2}. The only mineral-assemblage layers that may grow by diffusion-controlled reaction betwen quartz and dolomite are those across which there are nonzero gradients in the chemical potentials of one or more components. Local equilibrium thus limits permissible diffusion paths on the saturation surface between quartz and dolomite to those consisting of segments along the univariant edges TC + CC (Fig. 1A) or TR + CC (Fig. 2A), that link the invariant points, and segments that cross the divariant monomineralic planes, talc or tremolite, and calcite, that link univariant edges.

Layer sequences and diffusion paths in the quartz-talc-calcite-dolomite system

There are six additional layer sequences that may be derived from Q|TC + CC|DO by a shift of the chemical potentials off of one or both of the invariant points, Q|TC + CC and TC + CC|DO. Layer sequences that arise from a shift of the chemical potentials off of Q|TC + CC are Q|TC|TC + CC|DO and Q|CC|TC + CC|DO, whereas those derived by a shift of the μ's off of TC + CC|DO are Q|TC + CC|CC|DO and Q|TC + CC|TC|DO. A shift of the chemical potentials off of both invariant points leads to Q|TC|CC|DO and Q|CC|TC|DO.

Local equilibrium across three-phase layer contacts with quartz or dolomite results in invariant buffering at constant P-T-X_{CO_2}, so that values of μ_{CaO}, μ_{MgO}, and μ_{SiO_2} may be computed from Gibbs free energy data for the buffer assemblage containing three phases (+ fluid). Local equilibrium at layer contacts involving two phases, represented by a two-phase edge on the saturation surface, results in univariant buffering of the chemical potentials. Although the values of μ_{CaO}, μ_{MgO}, and μ_{SiO_2} in the univariant layer-contact assemblages are related by the Gibbs-Duhem equations for the two phases, their individual values cannot be computed directly from Gibbs free energy data.

The net differences in chemical potential across each of the seven possible layer sequences are such that chemical potentials at the layer contact with quartz are buffered to values that are higher for SiO_2 and lower for MgO than the corresponding potentials buffered at the layer contact with dolomite. Note that $\Delta\mu_{CaO} = 0$ across the CC and TC + CC layers because the presence of calcite fixes $\Delta\mu_{CaO}$ at its maximum value for the given P-T-X_{CO_2}. Thus CaO cannot diffuse across a calcite-bearing layer, unless there is a nonzero diffusion cross coefficient linking the flux of CaO with the gradient of μ_{MgO} or μ_{SiO_2}.

The shift of the chemical potentials from an invariant point to an adjacent univariant line causes the total difference in chemical potential between the quartz and dolomite layer contacts for each component to either increase or to remain unchanged, compared with its magnitude across Q|TC + CC|DO. The magnitude of $\Delta\mu_{MgO}$ is increased in structures with Q|CC, TC|DO, or both. The value of $\Delta\mu_{SiO_2}$ is increased in structures with a monomineralic layer at the dolomite layer contact, TC|DO or CC|DO. The value of $\Delta\mu_{CaO}$ is increased in structures with a monomineralic talc layer, Q|TC or TC|DO. Note that structures with the layer contact assemblage, Q|TC, buffer μ_{CaO} at the quartz contact to a value less than that of calcite saturation, whereas the layer contact assemblage, TC|DO, buffers μ_{CaO} at a value less than that of calcite saturation at the contact with dolomite.

Mineral-assemblage layers grow at one or both layer contacts by reaction between phases of the adjacent layers and components that diffuse down the gradient into the layer contact. Because $\Delta\mu_{CaO} = 0$ across any calcite-bearing layer, and because it is assumed that all cross coefficients linking the flux of one component to the chemical-potential gradient of another are zero, neither a monomineralic calcite layer nor a talc + calcite layer can grow at the layer contact with quartz in the model system. The only sequences of mineral-assemblage layers that may grow by diffusion-controlled reaction between quartz and dolomite in the model system are thus Q|TC + CC|DO, Q|TC|TC + CC|DO, and Q|TC|CC|DO. Which of these will actually grow is determined by the relative magnitudes of the diffusion fluxes of MgO and SiO_2.

Layer sequences and diffusion paths in the quartz-tremolite-calcite-dolomite system

Permissible diffusion paths linking quartz and dolomite on the saturation surface for the tremolite-bearing system (Fig. 2A) result in a set of seven layer sequences that are identical to those for the talc-bearing system, with the occurrence of tremolite in the place of talc. Net changes in $\Delta\mu_i$ are the same as those in the talc-bearing system for the corresponding univariant layer-contact buffers, Q|CC, CC|DO, and TR|DO. Buffering at the Q|TR layer contact results in an increase in $\Delta\mu_{CaO}$ and a decrease in $\Delta\mu_{MgO}$ relative to the values buffered across Q|TR + CC, whereas the value of $\Delta\mu_{SiO_2}$ is unchanged. Because $\Delta\mu_{CaO} = 0$ across TR + CC and CC layers, these layers cannot grow by diffusion-controlled reaction with quartz. The only layered structures that can grow in this system are thus, Q|TR + CC|DO, Q|TR|TR + CC|DO, and Q|TR|CC|DO. As before, the structure that will grow is determined by the magnitudes of the fluxes of CaO, MgO, and SiO_2.

Diffusion-controlled growth of talc-calcite and tremolite-calcite nodules

Local equilibrium and buffer reactions at layer contacts

Local equilibrium at a layer contact requires that the values of the chemical potentials of all components be those in equilibrium with the assemblages of the layers on both sides. Because material is continually supplied to and removed from the layer contact by diffusion, reaction must occur, consuming or producing diffusing components in the proportion that maintains local component concentrations and hence local chemical potentials at the values in equilibrium with the layer-contact assemblage. The buffering response is thus the growth of the assemblage of one layer by consumption of its neighbor and the consequent movement of the layer boundary. Stoichiometry of the reactions at layer contacts is controlled by the relative magnitudes of the fluxes of components diffusing into, and out of, the layer-contact reaction site.

Constrained mass balance model for diffusion-controlled growth of layered structures

Using the methods of nonequilibrium thermodynamics, Fisher (1973, 1975, 1977; also see Joesten, 1977; Nishiyama, 1983) developed a simple model describing the diffusion-controlled growth of layered structures in multicomponent, multiphase systems. In this model, the system of mass balance equations describing local equilibrium at mineral assemblage layer contacts,

$$\nu_i^{X|Y} = \sum_{i=1}^{n} n_i^X \nu_X^{X|Y} \tag{3}$$

is constrained by a set of conservation equations that link the stoichiometric coefficients of the layer-contact reactions to the diffusion fluxes in the adjacent layers,

$$\nu_i^{X|Y} = J_i^{X|OUT} - J_i^{Y|IN} \tag{4}$$

and a set of flux-ratio equations that constrain the diffusion fluxes in each layer to paths lying on the saturation surface,

$$J_i^X/J_j^X = L_{ii}d\mu_i^X/L_{jj}d\mu_j^X. \tag{5}$$

(The terms $\nu_i^{X|Y}$ and $\nu_x^{X|Y}$ are the stoichiometric coefficients for component i and phase X in the buffer reaction at the layer contact between assemblages comprising phases X and Y, n_i^X is the formula proportion of component i in phase X, $J_i^{X|OUT}$ and $J_i^{Y|IN}$ are the fluxes of component i in layers X and Y on the down-gradient and up-gradient sides of the $X|Y$ layer contact, and L_{ii} is the Onsager diffusion coefficient linking the flux of component i in layer X, J_i^X, to the chemical potential gradient $d\mu_i^X/dx$.)

Modeling diffusion-controlled growth of talc-calcite and tremolite-calcite nodules

Diffusion-controlled growth of model talc-calcite nodules with the structures Q|TC + CC|DO, Q|TC|TC + CC|DO, and Q|TC|CC|DO and tremolite-calcite nodules with the structures Q|TR + CC|DO, Q|TR|TR + CC|DO, and Q|TR|CC|DO is described by a system of mass balance equations for the components CaO, MgO, SiO_2, H_2O, and CO_2. Because Reactions 1 and 2 involve a net gain of H_2O and a net loss of CO_2 by the solids, these components are not included in the conservation equations. Because the system of mass balance, conservation, and flux-ratio equations that describe growth of the whole structure is underdetermined by one, it is necessary to specify the stoichiometric coefficient of one component or phase in the mass balance for one layer contact. Solutions for talc-calcite and tremolite-calcite nodules are thus scaled to the consumption of 4 mol and 8 mol of quartz, respectively. Solutions are then obtained by specifying values of the Onsager coefficient ratios (L_{ii}/L_{jj}) or "L-ratio") in the flux ratio equations. The values of $L_{H_2OH_2O/LSiO_2SiO_2}$ and $L_{CO_2CO_2}/L_{SiO_2SiO_2}$ were fixed at 1×10^6 for all models, to satisfy the assumption of constant X_{CO_2} across the structures.

The following strategy is used to determine the range of L-ratios over which a given talc-calcite or tremolite-calcite layer sequence is stable. A system of mass balance, conservation, and flux ratio equations is set up for a structure, such as Q|TC + CC|DO, and solved for arbitrary values of $L_{MgOMgO}/L_{SiO_2SiO_2}$ and $L_{CaOCaO}/L_{SiO_2SiO_2}$. If the sign of $\nu_X^{X/Y}$ for any phase is inconsistent with local equilibrium among the phases specified to coexist at that layer contact, then the layer sequence is considered to be unstable for that choice of L-ratios. Thus, Q|TC + CC|DO is unstable where calcite is consumed at Q|TC + CC and the structure Q|TC|TC + CC|DO is stable instead.

Note that the ratios $L_{MgOMgO}/L_{SiO_2SiO_2}$ and $L_{CaOCao}/L_{SiO_2SiO_2}$ have unique values that are a function of the values of the respective diffusion coefficients and concentrations of the components CaO, MgO, and SiO_2 in the intergranular network of the growing layers at a given P-T-X_{CO_2}. A close approximation to observed layer sequence, layer

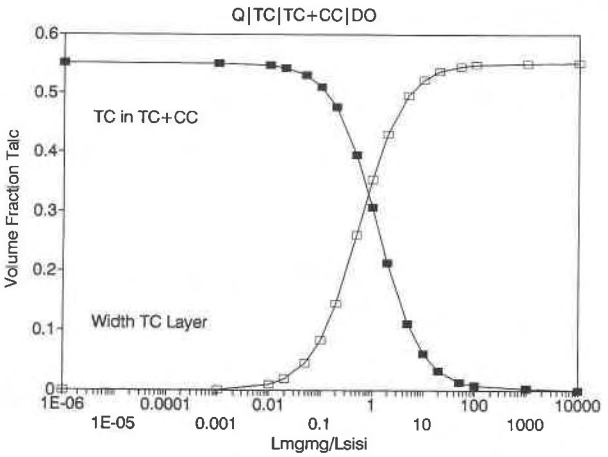

Fig. 3. Volume fraction of talc in a TC + CC layer (filled squares) and width of a TC layer as a fraction of the overall thickness of the Q|TC|TC + CC structure (open squares) as a function of $L_{MgOMgO}/L_{SiO_2SiO_2}$.

width, and modes of the two-phase layer by model calculation thus provides an estimate of $L_{MgOMgO}/L_{SiO_2SiO_2}$ and $L_{CaOCaO}/L_{SiO_2SiO_2}$ for the natural system. Although oxide components are used in the mass balance calculations, no inference is made as to the identity of the diffusing species in this system.

L-ratio, component fluxes, and stable layer sequences in talc-calcite nodules

Solutions for model talc-calcite nodules produced by reaction between quartz and dolomite were obtained for values of $L_{MgOMgO}/L_{SiO_2SiO_2}$ in the range 10^{-6} to 10^4 (Figs. 3 and 4A–4D). Because calcite grows only by reaction with dolomite, $J_{CaO} = 0$ ($\Delta\mu_{CaO} = 0$) across talc + calcite and calcite layers, and stoichiometry of individual layer-contact reactions is unaffected by variation in $L_{CaOCaO}/L_{SiO_2SiO_2}$. The layer sequence, Q|TC|TC + CC|DO, is the only structure that is diffusionally stable in this system. It is found, however, that the number of moles of talc formed by reaction with quartz at Q|TC ($\nu_{TC}^{Q|TC}$) exponentially approaches zero as $L_{MgOMgO}/L_{SiO_2SiO_2} \rightarrow 1 \times 10^{-6}$ and that the number of moles of talc formed by reaction with dolomite at TC + CC|DO ($\nu_{TC}^{TC+CC|DO}$) exponentially approaches zero as $L_{MgOMgO}/L_{SiO_2SiO_2} \rightarrow 1 \times 10^4$ (Fig. 3). Although the monomineralic talc layer in contact with quartz in Q|TC|TC + CC|DO does not truly vanish at low values of $L_{MgOMgO}/L_{SiO_2SiO_2}$, from an observational standpoint, the resulting structure effectively becomes Q|TC + CC|DO where $L_{MgOMgO}/L_{SiO_2SiO_2} \leq 10^{-6}$ because the value of $\nu_{TC}^{Q|TC}$ is less than 0.00002 mol talc per 4 mol of quartz consumed. Similarly, the structure effectively becomes Q|TC|CC|DO at high values of the L-ratio because $\nu_{TC}^{TC+CC|DO} \leq 0.00005$ mol talc per 4 mol quartz where $L_{MgOMgO}/L_{SiO_2SiO_2} \geq 10^4$.

Layer-contact reactions in Q|TC|TC + CC|DO, Q|TC + CC|DO, and Q|TC|CC|DO

Examples of the system of irreversible layer-contact reactions that describe diffusion-controlled growth of model talc-calcite nodules with the structures Q|TC + CC|DO, Q|TC|TC + CC|DO, and Q|TC|CC|DO are illustrated in Figure 4 for values of $L_{MgOMgO}/L_{SiO_2SiO_2} = 10^{-6}$, 0.1, 1, and 10^4. If it is assumed, as in the calculations illustrated in Figure 4, that the growing talc-calcite nodule is closed to diffusion of CaO, MgO, and SiO_2 beyond the layer contacts with quartz or dolomite, then quartz + dolomite will be consumed in the ratio 4 Q/3 DO and talc + calcite will be produced in the ratio 1 TC/3 CC. The following pair of mass balance equations expresses the stoichiometry of the irreversible layer-contact reactions:

$$4\ Q + 3X\ MgO + X\ H_2O \rightarrow X\ TC + 4(1 - X)\ SiO_2 \quad (6a)$$

at the quartz layer contact and

$$3\ DO + 4(1 - X)\ SiO_2 + (1 - X)H_2O \rightarrow (1 - X)\ TC + 3\ CC + 3X\ MgO + 3\ CO_2 \quad (6b)$$

at the dolomite layer contact, X is the fraction of the one mole of total talc that grows by reaction with quartz [$\nu_{TC}^{Q|TC} = 1 - 3/(3 + 4\ L_{MgOMgO}/L_{SiO_2SiO_2})$]. The sum of irreversible Reactions 6a and 6b is equivalent to reversible Reaction 1 and illustrates growth of structures with the layer sequence Q|TC|TC + CC|DO by counterdiffusion of MgO and SiO_2 where $0 < \nu_{TC}^{Q|TC} < 1$. There is no reaction at the TC|TC + CC layer contact, which represents the initial contact between quartz and dolomite.

Where $X = 0$, Reactions 6a and 6b are those that describe growth of the structure Q|TC + CC|DO (Fig. 4A). For $L_{MgOMgO}/L_{SiO_2SiO_2} \leq 10^{-6}$, $J_{MgO} \rightarrow 0$, and growth of a nodule with the structure Q|TC + CC|DO involves dissolution of 4 mol of quartz at Q|TC + CC and diffusion of 4 mol of SiO_2 down its chemical-potential gradient to TC + CC|DO, where it reacts with 3 mol of dolomite to produce 1 mol of talc + 3 mol of calcite (Fig. 4A). The initial contact between quartz and dolomite, represented by Q|TC + CC, migrates toward the core of the chert nodule as quartz is dissolved.

Where $X = 1$, Reactions 6a and 6b describe the growth of the structure Q|TC|CC|DO (Fig. 4D). Where $L_{MgOMgO}/L_{SiO_2SiO_2} \geq 10^4$, $J_{SiO_2} \rightarrow 0$, and 3 mol of calcite grow as a result of the breakdown of 3 mol of dolomite at CC|DO. Three moles of MgO released in the layer-contact reaction at CC|DO diffuse down its potential gradient to Q|TC, where they react with 4 mol of quartz to produce 1 mol of talc (Fig. 4D). There is no reaction at the TC|CC layer contact, which represents the initial boundary between quartz and dolomite.

Mode and layer width in Q|TC|TC + CC|DO

If the system is closed to gains or losses of CaO, MgO, and SiO_2 beyond the inner contact with quartz and the

outer contact with dolomite, the TC and TC + CC layers will contain talc and calcite in the molar proportion, 1 TC/3 CC given by the reversible Reaction 1. The actual modal proportions of talc and calcite in the TC + CC layer and the relative widths of the TC and TC + CC layers are determined by the relative fluxes of MgO and SiO_2 and hence by the ratio $L_{MgOMgO}/L_{SiO_2SiO_2}$. As the L-ratio is increased from 10^{-6} toward 10^4, the proportion of talc in the TC + CC layer decreases from 55.2 vol% toward 0 (mole fraction talc decreases from 0.25 to 0) and the width of the talc layer, as a fraction of the width of the overall structure, increases from 0 toward 0.552 (Figs. 4B–4D).

L-ratio, component fluxes, and stable layer sequences in model tremolite-calcite nodules

Solutions for tremolite-calcite nodules were obtained for values of $L_{MgOMgO}/L_{SiO_2SiO_2}$ in the range 10^{-6} to 10^4 and $L_{CaOCaO}/L_{SiO_2SiO_2}$ in the range 10^{-3} to 10^1 (Figs. 5A–5C, 6A–6D). Like the model talc-calcite nodules, the structure Q|TR|TR + CC|DO is diffusionally stable over the full range of values of $L_{MgOMgO}/L_{SiO_2SiO_2}$ and $L_{CaOCaO}/L_{SiO_2SiO_2}$ analyzed. Similarly, the value of $\nu_{TR}^{Q|TR}$ exponentially approaches zero as $L_{MgOMgO}/L_{SiO_2SiO_2} \rightarrow 1 \times 10^{-6}$ and $\nu_{TR}^{TR+CC|DO}$ exponentially approaches zero as $L_{MgOMgO}/L_{SiO_2SiO_2} \rightarrow 1 \times 10^4$, so that the structure Q|TR + CC|DO appears to be stable at low values of $L_{MgOMgO}/L_{SiO_2SiO_2}$ and Q|TR|CC|DO appears to be stable at high $L_{MgOMgO}/L_{SiO_2SiO_2}$.

Variation in $L_{CaOCaO}/L_{SiO_2SiO_2}$ determines the proportion of the monomineralic tremolite layer that grows by reaction with quartz at Q|TR and by reaction with calcite at TR|TR + CC (Figs. 5B and 5C). As $L_{CaOCaO}/L_{SiO_2SiO_2} \rightarrow 10$, $\nu_{TR}^{TR|TR+CC} \rightarrow 0$, essentially all tremolite in the monomineralic layer grows by reaction with quartz at Q|TR. Similarly, as $L_{CaOCaO}/L_{SiO_2SiO_2} \rightarrow 10^{-3}$, $\nu_{TR}^{Q|TR} \rightarrow 0$, essentially all tremolite in the monomineralic layer grows by reaction with calcite at TR|TR + CC.

If the system is closed to gains or losses of CaO, MgO, and SiO_2 beyond the inner contact with quartz and the outer contact with dolomite, the TR and TR + CC layers will contain tremolite and calcite in the molar proportion, 1 TR/3 CC, given by the reversible Reaction 2. As the ratio $L_{MgOMgO}/L_{SiO_2SiO_2}$ is increased from 10^{-6}, toward 10^4, the proportion of tremolite in the TR + CC layer decreases from 71.1 vol% toward 0 (mole fraction tremolite decreases from 0.25 to 0) and the width of the tremolite

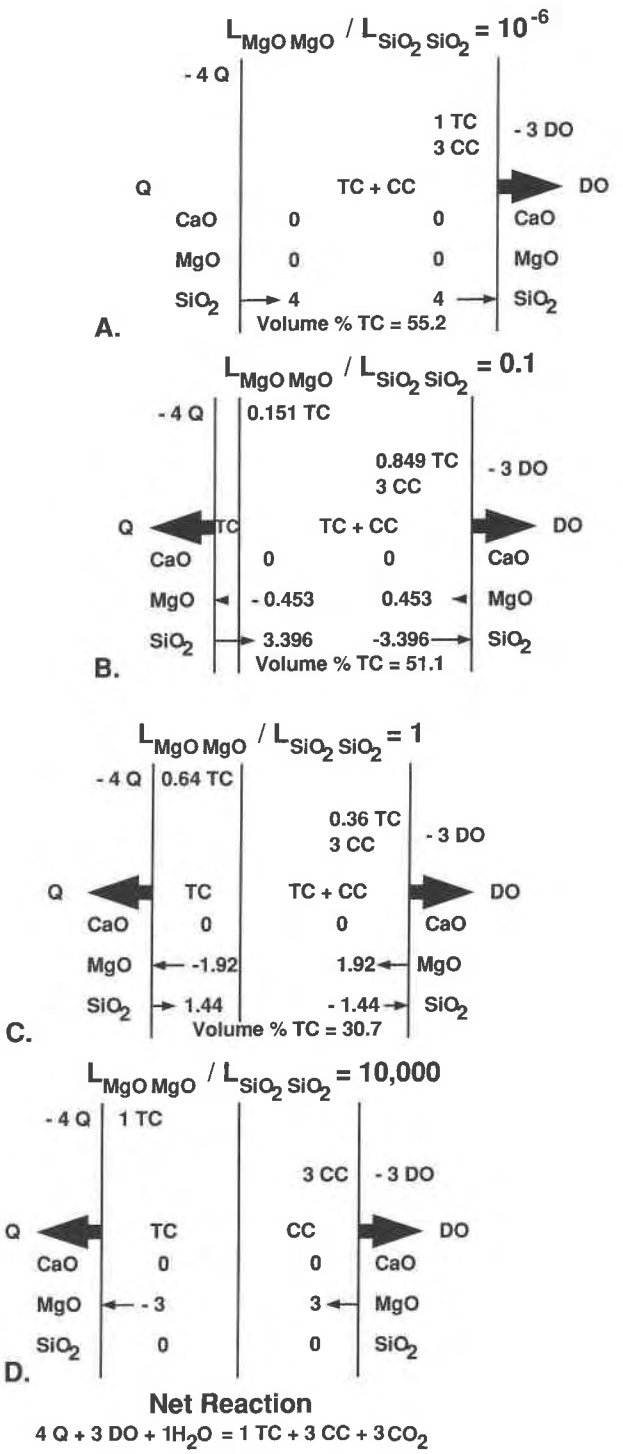

Fig. 4. Graphical portrayal of solutions to the system of mass balance, conservation, and flux ratio equations that describe growth of reaction rim(s) of talc-calcite initiated by Reaction 1 between dolomite and quartz. Solutions obtained for arbitrarily chosen values of $L_{MgOMgO}/L_{SiO_2SiO_2} = 10^{-6}$, 0.1, 1, and 10^4, with $L_{H_2OH_2O}/L_{SiO_2SiO_2} = L_{CO_2CO_2}/L_{SiO_2SiO_2} = 10^6$. Heavy arrows indicate direction of motion of layer contact as a result of production (+) or consumption (−) of phases on either side. Length of light arrows is proportional to the number of moles of CaO, MgO, or SiO_2 (ν_{CaO}, ν_{MgO}, and ν_{SiO_2}) evolved (+) or consumed (−) in layer contact reaction. Arrow points in direction of transport. Layer width scaled to the product of net number of moles of talc, calcite, or both in the layer and respective molar volumes. Models are aligned along the initial Q|DO layer contact, which coincides with Q|TC + CC in (**A**), TC|TC + CC in (**B**) and (**C**), and TC|CC in (**D**).

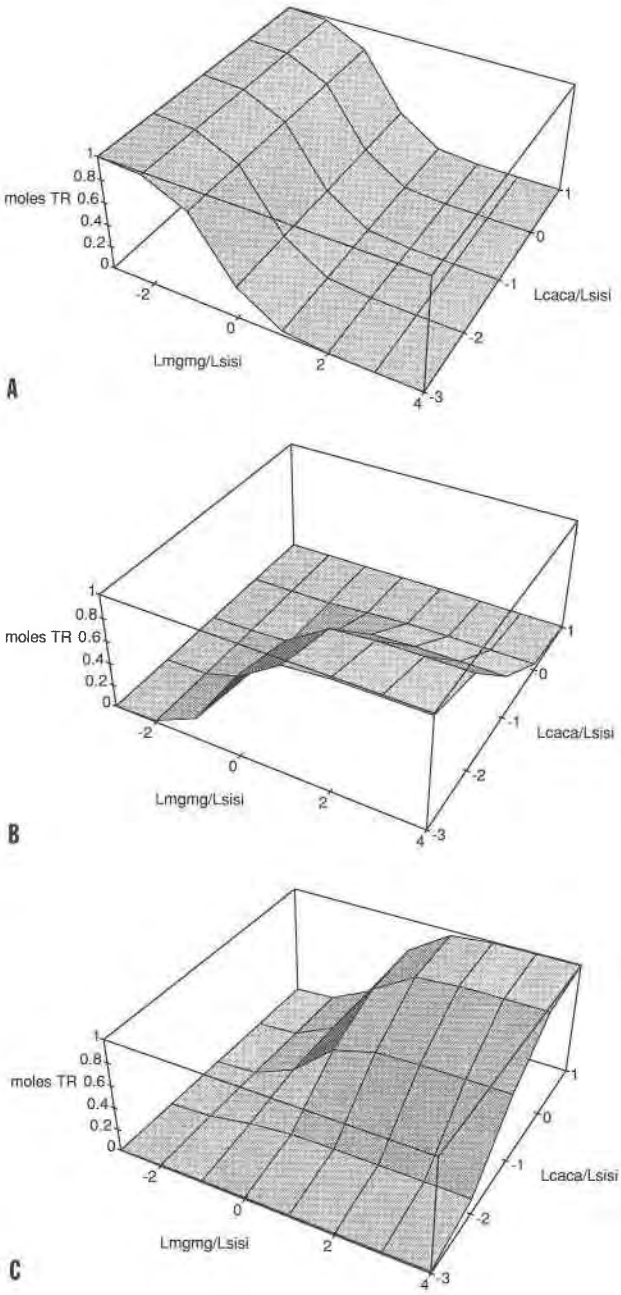

Fig. 5. Growth of tremolite (in moles) produced by diffusion-controlled reaction at TR + CC|DO (**A**), TR|TR + CC (**B**), and Q|TR (**C**) as a function of $\log_{10}L_{MgOMgO}/L_{SiO_2SiO_2}$ and $\log_{10}L_{CaOCaO}/L_{SiO_2SiO_2}$.

layer, as a fraction of the width of the overall structure, increases from 0 toward 0.711 (Figs. 6A–6D).

Diffusion-controlled reaction at the interior layer contact in model Q|TR|TR + CC|DO nodules

Model tremolite-calcite nodules with the layer sequence Q|TR|TR + CC|DO differ from their talc-calcite counterparts in the presence of a diffusion-controlled reaction at the TR|TR + CC layer contact (Figs. 6B–6D). Growth of tremolite by reaction with quartz at Q|TR consumes both CaO and MgO that must diffuse down gradient across the tremolite layer from their ultimate source at the TR + CC|DO contact. Shift of the chemical potentials from the Q + TR + CC invariant point to the Q + TR univariant edge results in a gradient in μ_{CaO} across the TR layer in Q|TR|TR + CC|DO (Figs. 2A and 2B). Note that because $\Delta\mu_{Cao} = 0$ across the TR + CC layer, all CaO consumed in the layer-contact reaction at Q|TR must be derived by the breakdown of calcite at TR|TR + CC (Figs. 6B–6D). Because the TR layer grows by the consumption of quartz at Q|TR and by the consumption of calcite at TR|TR + CC, the initial quartz-dolomite interface lies within the monomineralic tremolite layer (Figs. 6B–6D).

Stable steady state layer sequence

Surprisingly, the layer sequence Q|TR|CC|DO is diffusionally stable over the same range of $L_{MgOMgO}/L_{SiO_2SiO_2}$ and $L_{CaOCaO}/L_{SiO_2SiO_2}$ as Q|TR|TR + CC|DO. The simultaneous stability of two layer sequences that share a monomineralic layer in common, for an overlapping range of L-ratio, appears to be a characteristic feature of systems in which the amount of one of the product phases exponentially approaches zero with changing L-ratio. An explanation of this behavior in the tremolite-calcite system may lie in the fact that, for given values of $L_{MgOMgO}/L_{SiO_2SiO_2}$ and $L_{CaOCaO}/L_{SiO_2SiO_2}$, the stoichiometry of the layer contact reaction at Q|T is identical in both structures, so that component fluxes and chemical-potential gradients are the same in the monomineralic tremolite layer that they share in common.

The stoichiometric coefficients of the diffusing components in the layer contact reactions in the model structures represent the component fluxes that are attained in the steady state. Steady states play a role in the thermodynamic description of irreversible processes similar to that played by equilibrium states in equilibrium thermodynamics (Katchalsky and Curran, 1965). The steady state is characterized by minimization of the rate of local dissipation of free energy by irreversible processes. This is expressed by the requirement that the dissipation function,

$$T\sigma = \sum_{i=1}^{n} J_i \cdot (-\nabla\mu_i) \qquad (7)$$

representing the sum of the products of fluxes (J_i) and conjugate forces ($-\nabla\mu_i$), be minimized in the steady state (Katchalsky and Curran, 1965). Because the flux of component i is given by $J_i = L_{ii}(-\nabla\mu_i)$, Equation 7 may be written

$$T\sigma = \sum_{i=1}^{n} L_{ii}(-\nabla\mu_i^2) = \sum_{i=1}^{n} (J_i^2/L_{ii}). \qquad (8)$$

Although it has not been demonstrated that the dissipation function may be used to determine the relative

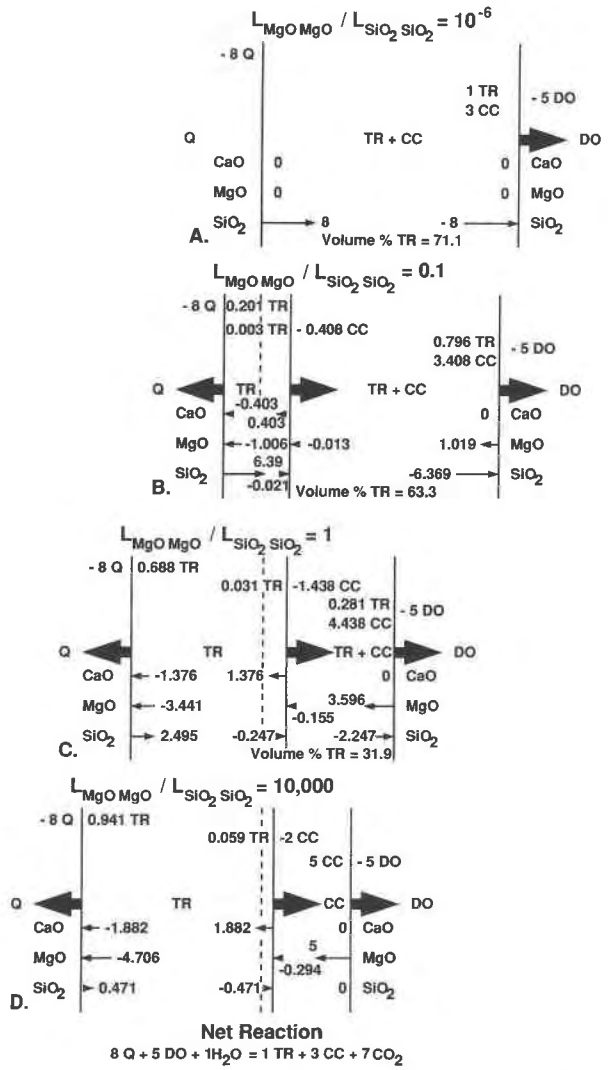

Fig. 6. Graphical portrayal of solutions to the system of mass balance, conservation, and flux ratio equations that describe growth of reaction rim(s) of tremolite-calcite initiated by Reaction 2 between dolomite and quartz. Solutions obtained for arbitrarily chosen values of $L_{MgOMgO}/L_{SiO_2SiO_2} = 10^{-6}$, 0.1, 1, and 10^4, with $L_{CaOCaO}/L_{SiO_2SiO_2} = 1$ and $L_{H_2OH_2O}/L_{SiO_2SiO_2} = L_{CO_2CO_2}/L_{SiO_2SiO_2} = 10^6$. Dashed line indicates initial Q|DO contact, the position is computed with Equation 10a in Joesten (1977). Models are aligned along the initial Q|DO contact. Notation as in Figure 4.

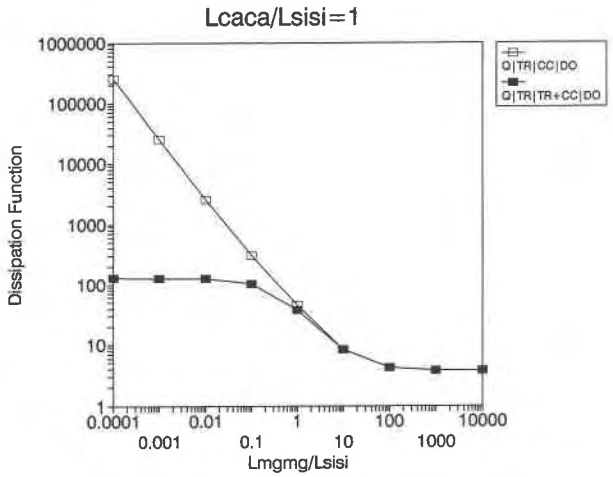

Fig. 7. Value of the dissipation function (Eq. 8) for the structures Q|TR|TR + CC|DO (filled squares) and Q|TR|CC|DO (open squares) as a function of $L_{MgOMgO}/L_{SiO_2SiO_2}$ for $L_{CaOCaO}/L_{SiO_2SiO_2} = 1$.

stability of two steady states, it seems plausible that the stable steady state is the one with the smaller value of $T\sigma$. Values of the right-hand equality in Equation 8 have been calculated for the structures Q|TR|TR + CC|DO and Q|TR|CC|DO as a function of $L_{MgOMgO}/L_{SiO_2SiO_2}$ and $L_{CaOCaO}/L_{SiO_2SiO_2}$ (Fig. 7). Note that the value of $T\sigma$ for Q|TR|TR + CC|DO is smaller than that for Q|TR|CC|DO, where $L_{MgOMgO}/L_{SiO_2SiO_2} \leq 10$, but values converge for $L_{MgOMgO}/L_{SiO_2SiO_2} \approx 100$–1000. In this range, the value of $\nu_{TR}^{TR+CC|DO}$ is in the range 0.004–0.0004 and volume fraction tremolite is 0.006–0.0006, so that the TR + CC layer is effectively monomineralic in calcite. The layer sequence Q|TR|TR + CC|DO is thus believed to represent the stable steady state over the range $10^{-6} \leq L_{MgOMgO}/L_{SiO_2SiO_2} \leq 10^4$.

Comparison of model talc-calcite and tremolite-calcite nodules with natural examples

Nodules from the talc and tremolite zones in the Alta aureole have the layer sequence Q|TC + CC|DO and Q|TR + CC|DO (Moore and Kerrick, 1976), consistent with $L_{MgOMgO}/L_{SiO_2SiO_2} \leq 10^{-6}$. Although the mineral assemblages of similar nodules from the Beinn an Dubhaich aureole are complicated by the presence of tremolite, talc, or both in both the quartz core and the dolomite matrix as a result of impurities in the chert and dolostone (Hoersch, 1981), structures of nodules from the talc and tremolite zones may be interpreted as approximating Q|TC + CC|DO and Q|TR + CC|DO. Using a procedure similar to that developed here, but making use of measured modes of mineral-assemblage layers to solve for L_{ii}/L_{jj}, Hoersch (1979) computed $L_{MgOMgO}/L_{SiO_2SiO_2} = 0.08$ for the talc zone and $L_{MgOMgO}/L_{SiO_2SiO_2} = 0.05$ for the tremolite zone. Note that the width of the talc layer in Q|TC|TC + CC|DO and of the TR layer in Q|TR|TR + CC|DO decreases rapidly as $L_{MgOMgO}/L_{SiO_2SiO_2}$ is decreased below 0.1, and that a thin monomineralic talc or tremolite layer may be easily overlooked. The results of model calculations and petrographic studies are consistent with $L_{MgOMgO}/L_{SiO_2SiO_2} < 0.1$. Hoersch (1979) computed $L_{CaOCaO}/L_{SiO_2SiO_2} = 0.01$ for the talc zone and $L_{CaOCaO}/L_{SiO_2SiO_2} = 0.05$ for the tremolite zone. The criterion for estimation of $L_{CaOCaO}/L_{SiO_2SiO_2}$ in the model system is the position of a textural boundary within the monomineralic talc or tremolite layer that represents the initial Q|DO contact. Because monomineralic layers are not observed at Beinn an Dubhaich, the value of $L_{CaOCaO}/L_{SiO_2SiO_2}$ cannot be estimated from them using the model presented here.

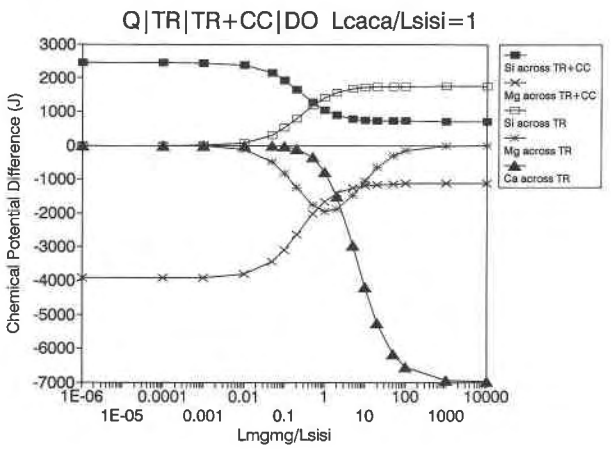

Fig. 8. Chemical potential differences for CaO, MgO, and SiO_2 across the TR and TR + CC layers, defined as $\Delta\mu_i^{TR} = (\mu_i^{Q|TR} - \mu_i^{TR|TR+CC})$ and $\Delta\mu_i^{TR+CC} = (\mu_i^{TR|TR+CC} - \mu_i^{TR+CC|DO})$, as a function of $L_{MgOMgO}/L_{SiO_2SiO_2}$ for $L_{CaOCaO}/L_{SiO_2SiO_2} = 1$ for conditions of 450 °C, 500 bars, and $X_{CO_2} = 0.9$ (see text).

Chemical potential gradients in model tremolite-calcite nodules

Calculation of μ_{CaO}, μ_{MgO}, and μ_{SiO_2} at univariant layer contacts

The invariant (at fixed T, P, and X_{CO_2}) assemblages of layer contacts Q|TR + CC and TR + CC|DO buffer μ_{CaO}, μ_{Mgo}, and μ_{SiO_2} to values that may be calculated using Gibbs free energy data for the phases. Values of μ_{CaO}, μ_{MgO}, and μ_{SiO_2} at the univariant layer contacts TR|TR + CC and Q|TR are obtained by extrapolation from values calculated from thermochemical data using component fluxes and layer widths computed as a function of L-ratio in the model structure.

For Q|TR|TR + CC|DO, values of $\mu_{CaO}^{TR+CC|DO}$ (= $\mu_{CaO}^{TR|TR+CC}$), $\mu_{MgO}^{TR+CC|DO}$, $\mu_{SiO_2}^{TR+CC|DO}$ are computed from thermochemical data. It is assumed that values of $d\mu_{SiO_2}/dx$ and $d\mu_{MgO}/dx$ in the TR + CC layer are identical to those across Q|TR + CC|DO. This results in identical potential gradients for SiO_2 in both the TR and TR + CC layers. Values of $\mu_{MgO}^{TR|TR+CC}$ and $\mu_{SiO_2}^{TR|TR+CC}$ at the univariant interior layer contact are then obtained by linear extrapolation,

$$\mu_{MgO}^{TR|TR+CC} = \mu_{MgO}^{TR+CC|DO} + (d\mu_{MgO}/dx)^{TR+CC} W^{TR+CC} \quad (9a)$$

and

$$\mu_{SiO_2}^{TR|TR+CC} = \mu_{SiO_2}^{TR+CC|DO} + (d\mu_{SiO_2}/dx)^{TR+CC} W^{TR+CC} \quad (9b)$$

where W^{TR+CC} is the width of the TR + CC layer computed from the mass balance for a given value of $L_{MgOMgO}/L_{SiO_2SiO_2}$. Values of $\mu_{CaO}^{Q|TR}$ and $\mu_{MgO}^{Q|TR}$ are then obtained from the flux-ratio equations

$$\mu_{CaO}^{Q|TR} = \mu_{CaO}^{TR|TR+CC}\left[\frac{\nu_{CaO}^{Q|TR}}{\nu_{SiO_2}^{Q|TR}}\right]\left[\frac{L_{SiO_2SiO_2}}{L_{CaOCaO}}\right] \cdot(\mu_{SiO_2}^{Q|TR} - \mu_{SiO_2}^{TR|TR+CC}) \quad (10a)$$

and

$$\mu_{MgO}^{Q|TR} = \mu_{MgO}^{TR|TR+CC}\left[\frac{\nu_{MgO}^{Q|TR}}{\nu_{SiO_2}^{Q|TR}}\right]\left[\frac{L_{SiO_2SiO_2}}{L_{MgOMgO}}\right] \cdot(\mu_{SiO_2}^{Q|TR} - \mu_{SiO_2}^{TR|TR+CC}). \quad (10b)$$

Differences in the chemical potentials for CaO, MgO, and SiO_2 across the TR and TR + CC layers, defined as $\Delta\mu_i^{TR} = (\mu_i^{Q|TR} - \mu_i^{TR|TR+CC})$ and $\Delta\mu_i^{TR+CC} = (\mu_i^{TR|TR+CC} - \mu_i^{TR+CC|DO})$, are plotted as a function of $L_{MgOMgO}/L_{SiO_2SiO_2}$ for $L_{CaOCaO}/L_{SiO_2SiO_2} = 1$ in Figure 8 for conditions of 450 °C, 500 bars, and $X_{CO_2} = 0.9$. Shift of the chemical potentials from the Q + TR + CC invariant point on the saturation surface to the Q + TR univariant edge as $L_{MgOMgO}/L_{SiO_2SiO_2}$ is increased, results in a decrease in the value of $\mu_{MgO}^{Q|TR}$ relative to $\mu_{MgO}^{Q|TR+CC}$ and the establishment of a chemical potential gradient for CaO across the tremolite layer. The magnitude of $\Delta\mu_{CaO}^{TR}$ increases from zero to −6968 J/mol as $L_{MgOMgO}/L_{SiO_2SiO_2}$ is increased from 10^{-6} to 10^4. The gradient of μ_{CaO} is zero across the TR + CC layer because calcite fixes μ_{CaO} throughout the layer at constant P-T-X_{CO_2}.

Growth of the monomineralic tremolite layer, and its progressive widening with increasing $L_{MgOMgO}/L_{SiO_2SiO_2}$ over the range 10^{-6} to 10^4, results in a progressive decrease in $\Delta\mu_{MgO}$ across the Q|TR|TR + CC|DO structure, from −3923 J/mol to −1135 J/mol and exponential variation in $\Delta\mu_{MgO}^{TR}$ from zero, through a maximum of −1948 J/mol at $L_{MgOMgO}/L_{SiO_2SiO_2} = 1$ and back to zero. The maximum in $\Delta\mu_{MgO}^{TR}$ arises because both $\mu_{MgO}^{TR+CC|DD}$ and $\mu_{MgO}^{TR|TR+CC}$ vary exponentially between minimum and maximum values with increasing L-ratio.

Variation in $L_{CaOCaO}/L_{SiO_2SiO_2}$ from 10^{-3} to 10^1 results in (1) a shift of the steeply sloping leg of the $\Delta\mu_{CaO}^{TR}$ curve to higher $L_{MgOMgO}/L_{SiO_2SiO_2}$ while its maximum value remains unchanged, (2) an increase in the maximum in $\Delta\mu_{MgO}^{TR}$ and its shift to higher values of $L_{MgOMgO}/L_{SiO_2SiO_2}$, and (3) no change in the values of $\Delta\mu_{SiO_2}^{TR+CC}$, $\Delta\mu_{SiO_2}^{TR}$, and $\Delta\mu_{MgO}^{TR+CC}$.

Flux divergence and the stoichiometry of layer-contact reactions

Reaction at the interior layer contact in Q|TR|TR + CC|DO illustrates the relationship between consumption or production of diffusing components in a layer-contact reaction and the consequent changes their chemical-potential gradients at the layer contact (Fig. 9). Where a component is consumed in a layer-contact reaction, as is MgO at TR|TR + CC and Q|TR, the gradient flattens in the direction of transport. Where a component is evolved in a layer-contact reaction, as is MgO at TR + CC|DO, the gradient steepens in the direction of transport.

Diffusion path linking univariant layer contacts in Q|TR|TR + CC|DO

In the steady state, differences in the total chemical potential across a layered structure adjust in an attempt

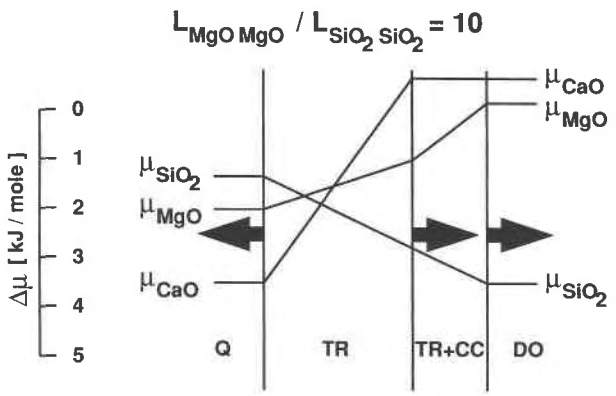

Fig. 9. Values of μ_{CaO}, μ_{MgO}, and μ_{SiO_2} buffered at invariant and univariant layer contacts calculated at 450 °C, 500 bars, and $X_{CO_2} = 0.9$ for model structures computed for $L_{MgOMgO}/L_{SiO_2SiO_2} = 10$ (see text). Values are normalized to an arbitrary origin at TR + CC|DO and gradients within layers are assumed to be constant. Layer width scaled as in Figure 6.

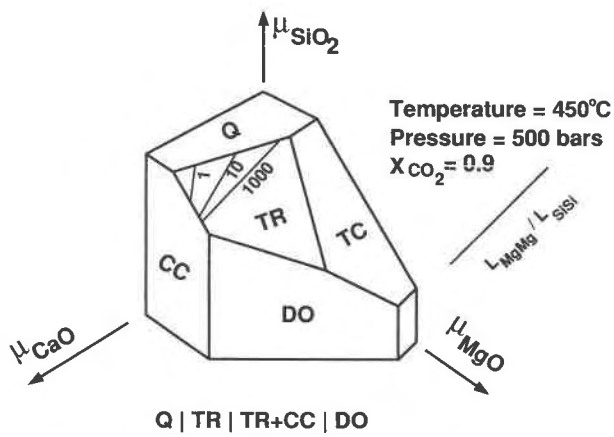

Fig. 10. Diffusion paths linking the univariant edges Q + TR and TR + CC across the plane of tremolite saturation on the μ_{CaO}-μ_{MgO}-μ_{SiO_2} saturation surface, illustrating the decrease in $\Delta\mu_{MgO}$ across TR with increasing $L_{MgOMgO}/L_{SiO_2SiO_2}$ for $L_{CaOCaO}/L_{SiO_2SiO_2} = 1$. End points of lines are given by values of μ_{CaO}, μ_{MgO}, and μ_{SiO_2} buffered by univariant equilibria at the Q|TR and TR|TR + CC layer contacts, calculated using Gibbs free energy data at 450 °C, 500 bars, and $X_{CO_2} = 0.9$ and using layer widths calculated for $L_{MgOMgO}/L_{SiO_2SiO_2} = 1$, 10, and 1000 (see text).

to balance the fluxes of diffusing components by increasing the driving force for the diffusion of components with small values of the Onsager diffusion coefficient, and decreasing the driving force for components with large values of L_{ii}. Growth of a monomineralic tremolite layer at Q|TR in Q|TR|TR + CC|DO forces the chemical potentials off of the Q + TR + CC invariant point and onto the Q + TR and TR + CC univariant lines, thus decreasing the difference of the total chemical potential for MgO across the structure relative to that buffered by the two invariant points (Fig. 10).

A set of diffusion paths across the tremolite plane on the saturation surface may be illustrated by linking the values of μ_{CaO}, μ_{MgO}, and μ_{SiO_2} buffered by the univariant assemblages, Q + TR at Q|TR and TR + CC at TR|TR + CC, and the invariant assemblage at TR + CC|DO, for values of $L_{MgOMgO}/L_{SiO_2SiO_2} = 1$, 10, and 1000 (Fig. 10). Shift of the chemical potentials off of the Q + TR + CC invariant point with increasing $L_{MgOMgO}/L_{SiO_2SiO_2}$ results in an overall decrease in $\Delta\mu_{MgO}$ across the Q|TR|TR + CC|DO structure. The magnitude of $\Delta\mu_{MgO}$ across the tremolite layer decreases and the magnitude of $\Delta\mu_{SiO_2}$ across TR increases as $L_{MgOMgO}/L_{SiO_2SiO_2}$ is increased. Shift of the chemical potentials onto the Q + TR edge also results in a finite chemical-potential gradient for CaO across the tremolite layer that increases with $L_{MgOMgO}/L_{SiO_2SiO_2}$, so that CaO evolved by the consumption of calcite at TR|TR + CC can diffuse down its potential gradient across the tremolite layer to be consumed in the tremolite-producing reaction at Q|TR.

Number of perfectly mobile components and number of diffusing components in layered structures

The model nodules of talc-calcite and tremolite-calcite illustrated in Figures 4 and 6 provide revealing illustrations of the absence of a consistent relationship between component mobility in the context of the phase rule and component mobility in the context of mass transport.

Mineral assemblage variance and the number of perfectly mobile components in talc-calcite, tremolite-calcite, and monomineralic layers

As shown on the saturation surface for μ_{CaO}-μ_{MgO}-μ_{SiO_2} at fixed P-T-X_{CO_2} for these systems (Figs. 1A and 2A) there is one independently variable chemical potential in the two-phase layer TC + CC in Q|TC + CC|DO and Q|TC|TC + CC|DO and in the two-phase layer TR + CC in Q|TR + CC|DO and Q|TR|TR + CC|DO. In the context of the phase rule, one component is perfectly mobile (Korzhinskii, 1959) or behaves as a K component (Thompson, 1970) within TC + CC and TR + CC. If we consider the two-phase layer to be the local system, then the chemical potential of the K component is controlled "external to the local system" by invariant or univariant local buffer equilibria at the layer contacts bounding it on either side (Q|TC + CC or TC|TC + CC and TC + CC|DO, and Q|TR or TR|TR + CC and TR + CC|DO), as are the chemical potentials of the other two components. The remaining two components are inert or J components because the ratio of their potential gradients in the TC + CC or TR + CC layer must simultaneously satisfy the Gibbs-Duhem equations for calcite and talc or tremolite. The number of perfectly mobile or K components is equal to the variance (at fixed P-T-X_{CO_2}) in mineral-assemblage layers that have grown by diffusion-controlled reaction because the range of accessible values of the chemical potentials within the layer is imposed by buffer equilibria at the layer contacts.

Because the chemical potential of CaO is fixed by the

presence of calcite in the univariant layer, CaO is an inert or J component in that layer. The value of either μ_{MgO} or μ_{SiO_2} may thus be independently varied in TC + CC and TR + CC, so that either MgO or SiO_2 may be a perfectly mobile or K component, whereas the other is an inert or J component in these layers.

Chemical potentials within the divariant talc, tremolite, and calcite layers may vary between the limits imposed by univariant buffer equilibria at their layer contacts. Thus, any two of the three components, CaO, MgO, and SiO_2 may perfectly mobile or K components wtihin the talc or tremolite layer, whereas CaO must be an inert or J component in the calcite layer and both MgO and SiO_2 are K components.

Number of diffusing components in univariant and divariant layers

There is a single diffusing component, SiO_2, in the TC + CC and TR + CC layers of limiting structures, Q|TC + CC|DO and Q|TR + CC|DO, as might be expected in a univariant layer. Both MgO and SiO_2 diffuse through TC + CC and TR + CC in Q|TC|TC + CC|DO and Q|TR|TR + CC|DO, however.

One, two, or three components are observed to diffuse through divariant monomineralic layers in the model structures. MgO diffuses through calcite in Q|TC|CC|DO and Q|TR|CC|DO and SiO_2 diffuses through tremolite in Q|TR|CC|DO at $L_{CaOCaO}l/L_{SiO_2SiO_2} \leq 10^{-3}$. MgO and SiO_2 diffuse through talc in Q|TC|TC + CC|DO, whereas CaO and MgO diffuse through tremolite in Q|TR|CC|DO at $L_{CaOCaO}l/L_{SiO_2SiO_2} \geq 10^{1}$. All three components diffuse through the divariant tremolite layer in Q|TR|TR + CC|DO.

The number of diffusing components has been shown in these examples to be greater than, equal to, or less than the number of perfectly mobile or K components in a given layer. The model structures of talc-calcite and tremolite-calcite serve as a reminder that the number of perfectly mobile or K components in a mineral-assemblage layer and the number of components that diffuse through the layer are only coincidentally related (Thompson, 1970; Joesten, 1974; Brady, 1977), and they demonstrate that the number of components diffusing through a layer cannot be predicted from the variance of the layer assemblage. Korzhinskii's (1950, 1959) choice of the terms, "perfectly mobile" and "inert," to describe component behavior in metasomatic rocks was unfortunate because it may cause the unwary to equate "phase rule mobility" with "mass transport mobility," as has been pointed out by Thompson (1970) and Rumble (1982).

Postscript

The concept of the buffering of chemical potentials by local equilibrium at layer contacts, proposed by Thompson in "Local Equilibrium in Metasomatic Processes" (1959) and elegantly illustrated in "Geochemical Reaction and Open Systems" (1970), is the heart and soul of this contribution. Although we who worry about the modeling of the mass transport in metamorphic rocks rarely mention perfectly mobile and inert components or K and J components, the ideas that Thompson developed using them are crucial to our enterprise because they focused our attention on the problem of the origin high-variance assemblages. Everything else follows from that.

Acknowledgments

I thank John Brady, Alice Hoersch, Cambria Johnson, and Bill Carlson for thought-provoking comments that significantly improved the clarity of the final manuscript. In the course of comparing my results with those computed with their program, Bill and Cambria discovered the overlap of stability fields on the L-ratio plane for structures with exponential variation in amount of a product phase. The support of NSF EAR-88-17254 is gratefully acknowledged.

References cited

Brady, J.B. (1977) Metasomatic zones in metamorphic rocks. Geochimica et Cosmochimica Acta, 41, 113–125.

Fisher, G.W. (1973) Nonequilibrium thermodynamics as a model for diffusion-controlled metamorphic processes. American Journal of Science, 273, 897–924.

——— (1975) The thermodynamics of diffusion controlled metamorphic processes. In A.R. Cooper and A.H. Heuer, Eds., Mass transport phenomena in ceramics, p. 111–122. New York, Plenum Press.

——— (1977) Nonequilibrium thermodynamics in metamorphism. In D.G. Fraser, Ed., Thermodynamics in geology, p. 381–403. Reidel, Dordrecht, Holland.

Flowers, G.C. (1979) Correction to Holloway's adaptation of the modified Redlich-Kwong equation of state for calculation of the fugacities of molecular species in supercritical fluids of geologic interest. Contributions to Mineralogy and Petrology, 69, 315–318.

Frantz, J.D., and Mao, H.K. (1975) Bimetasomatism resulting from intergranular diffusion: Multimineralic zone sequences. Carnegie Institution of Washington Year Book, 74, 417–424.

——— (1979) Bimetasomatism resulting from intergranular diffusion: II. Prediction of multimineralic zone sequences. American Journal of Science, 279, 302–323.

Grant, J.A. (1977) Crystallographic projection of chemical potential relationships as an aid in the interpretation of metasomatic zoning. American Mineralogist, 62, 1012–1017.

Helgeson, H.C., Delany, J.M., Nesbitt, H.W., and Bird, D.K. (1978) Summary and critique of the thermodynamic properties of rock-forming minerals. American Journal of Science, 278A, 1–229.

Hoersch, A.L. (1979) Diffusion-controlled growth of layered calc-silicate nodules. Geological Society of America Abstracts with Programs, 11, 444.

——— (1981) Progressive metamorphism of the chert-bearing Durness limestone in the Beinn an Dubhaich aureole, Isle of Skye, Scotland: A reexamination. American Mineralogist, 66, 491–506.

Holloway, J.R. (1977) Fugacity and activity of molecular species in supercritical fluids. In D.G. Fraser, Ed., Thermodynamics in geology, p. 161–181. Reidel, Dordrecht, Holland.

Joesten, R. (1974) Local equilibrium and metasomatic growth of zoned calc-silicate nodules from a contact aureole, Christmas Mountains, Big Bend Region, Texas. American Journal of Science, 274, 876–901.

——— (1977) Evolution of mineral assemblage zoning in diffusion metasomatism. Geochimica et Cosmochimica Acta, 41, 649--670.

——— (1983) Grain growth and grain boundary diffusion in quartz from the Christmas Moutains, Texas, contact aureole. American Journal of Science, 283A (Orville Volume), 233–254.

Joesten, R., and Fisher, G.W. (1988) Kinetics of diffusion-controlled mineral growth in the Christmas Moutains (Texas) contact aureole. Geological Society of America Bulletin, 100, 714–732.

Katachalsky, A., and Curran, P.F. (1965) Nonequilibrium thermodynamics in biophysics, 248 p. Harvard University Press, Cambridge, Massachusetts.

Korzhinskii, D.S. (1950) Phase rule and geochemical mobility of elements. 18th International Geological Congress (Great Britain) Report, Part 2, 50–65.

——— (1959) Physicochemical basis of the analysis of the paragenesis of minerals, 142 p. Consultants Bureau, New York.

——— (1966) On thermodynamics of open systems and the phase rule (A reply to D.F. Weill and W.S. Fyfe). Geochimica et Cosmochimica Acta, 30, 829–835.

——— (1967) On thermodynamics of open systems and the phase rule (A reply to the second critical paper of D.F. Weill and W.S. Fyfe). Geochimica et Cosmochimica Acta, 31, 1177–1180.

Moore, J.N., and Kerrick, D.M. (1976) Equilibria in siliceous dolomites of the Alta aureole, Utah. American Journal of Science, 276, 502–524.

Nishiyama, T. (1983) Steady diffusion model for olivine-plagioclase corona growth. Geochimica et Cosmochemica Acta, 47, 283–294.

Puga, E., and Fontboté, J.M. (1980) Zoned silicate nodules in brucite marble, Santa Olalla, western Sierra Morena, Spain. Schweizerisch Mineralogische und Petrographische Mitteilungen, 60, 69–80.

Reverdatto, V.V. (1970) Pyrometamorphism of limestones and the temperature of basaltic magmas. Lithos, 3, 135–143.

Rumble, D., III (1982) The role of perfectly mobile components in metamorphism. Annual Reviews of Earth and Planetary Science, 10, 221–233.

Suzuki, K. (1977) Local equilibrium during the contact metamorphism of siliceous dolomites in Kasuga-mura, Gifu-ken, Japan. Contributions to Mineralogy and Petrology, 61, 79–89.

Thompson, J.B., Jr. (1959) Local equilibrium in metasomatic processes. Researches in geochemistry, 1, 427–457.

——— (1970) Geochemical reaction and open systems. Geochimica et Cosmochimica Acta, 34, 525–551.

Tilley, C.E. (1942) Tricalcium disilicate (rankinite), a new mineral from Scawt Hill, Co. Antrim. Mineralogical Magazine, 26, 190–196.

——— (1948) Earlier stages in the metamorphism of siliceous dolomites. Mineralogical Magazine, 28, 272–276.

——— (1951) The zoned contact-skarns of the Broadford area, Skye: A study of boron-fluorine metasomatism in dolomites. Mineralogical Magazine, 29, 621–666.

Tilley, C. E., and Alderman, A.R. (1934) Progressive metasomatism in the flint nodules of the Scawt Hill contact zone. Mineralogical Magazine, 23, 513–518.

Walther, J.V. (1983) Description and interpretation of metasomatic phase relations at high pressure and temperature: 2. Metasomatic reactions between quartz and dolomite at Campolungo, Switzerland. American Journal of Science, 283A (Orville Volume), 459–485.

Walther, J.V., and Helgeson, H.C. (1980) Description and interpretation of metasomatic phase relations at high pressure and temperature: 1. Equilibrium activities of ionic species in nonideal mixtures of CO_2 and H_2O. American Journal of Science, 280, 575–606.

Weill, D.F., and Fyfe, W.S. (1964) A discussion of the Korzhinskii and Thompson treatment of thermodynamic equilibrium in open systems. Geochimica et Cosmochimica Acta, 28, 565–576.

——— (1967) On equilibrium thermodynamics of open systems and the phase rule (A reply to D.S. Korzhinskii). Geochimica et Cosmochimica Acta, 31, 1167–1176.

Manuscript received February 1, 1990
Manuscript accepted February 12, 1991